Thermal Model of a Ball Bearing using the State-Space approach and Light Gray-Box Lumped Parameter Thermal Network

Sebastian Cabezas[1*], *Dániel* Tóth[2], *György Hegedűs*[3] and *Péter* Bencs[4]

[1]Institute of Machine Tools and Mechatronics, Faculty of Mechanical Engineering and Information Technology, University of Miskolc, Miskolc-Egyetemváros, Hungary, Email: szgtscab@uni-miskolc.hu.
[2,3] Institute of Machine Tools and Mechatronics, Faculty of Mechanical Engineering and Information Technology, University of Miskolc, Miskolc-Egyetemváros, Hungary, Email: hegedus.gyorgy@uni-miskolc.hu, Email: daniel.toth1@uni-miskolc.hu
[4] Institute of Energy Engineering and Chemical Machinery, Faculty of Mechanical Engineering and Information Technology, University of Miskolc, Miskolc-Egyetemváros, Hungary, Email: peter.bencs@uni-miskolc.hu

Abstract. In this paper, a thermal model of a ball bearing subjected to radial loads is presented. By the application of the State-Space approach and the Light Gray-Box lumped parameter thermal network, the temperature of the inner components of a ball bearing, these are: outer-race T_o; balls T_b and inner-race T_i; and the temperature of the housing T_h were determined. The relation between the external force, rotational speed, lubrication type, were investigated for the purpose of determining the total frictional moment M_f that occurs among the elements comprising the ball bearing. Subsequently, the total heat losses $\dot{Q}_f$ were calculated together with the heat distribution along the elements of the ball bearing. The analytical results were validated experimentally. It could be seen that the standard deviation of temperature between the thermal model and the experimental measurements over the outer-race T_o and housing T_h were $sd = 5.06\,\%$ and $sd = 0.33\,\%$. Moreover, the temperature of the balls T_b and the inner-race T_i were predicted. In this context, the results show good agreement with real data, therefore, the thermal model can be utilized to foresee the thermal behavior of bearings with similar geometry that undergo effects of radial loads.

Keywords: Thermal model, State-Space approach, Light Gray-Box lumped parameter thermal network, ball bearing.

* Corresponding author: szgtscab@uni-miskolc.hu

1 Introduction

Ball bearings are mechanical components that can be found practically in every machine or mechanism involving rotational movement. In fact, their proper functioning directly influences the performance of a machine. Among the factors that might lead to an inadequate functionality of a ball bearing is the thermal behavior thereof, which is characterized by internal aspects including, friction between the balls and races, the type and regime of lubrication; and external factors including, the type of the applied load, the rotational speed, the type of bearing arrangement, among others. Over time, significant contributions regarding the investigation of the thermal analysis in bearings have been conducted, thus, revealing issues that can be avoided or diminished in order to guarantee a suitable performance of ball bearings and adjacent elements. Nevertheless, the determination of the temperature paths and temperature distribution within the elements of a rolling bearing is still an issue that demands attention. The techniques and methods to determine the thermal behavior of a bearing include analytical and experimental approaches. Certainly, the analytical approach presents more complexity, as it involves the solution of cumbersome mathematical formulations. In contrast, the experimental approach could be more consistent, since real data can be obtained; nevertheless, the cost of performing an experiment represents a considerable impediment. The most suitable method to determine the thermal behavior of ball bearings is the combination of experimental and analytical approaches. To mention some remarkable contributions on this field, Hoffman F. et al [1], presented a thermal model speed-dependent and speed-independent thermal ball resistance, being able to determine accurately the temperature distribution of a ball bearing, however, no experimental validation has been performed. Takabi J. et al [2], presented a comprehensive mathematical model to analyze the thermal behavior in ball bearings in steady- and transient-state applicable for a wide range of ball bearings. By experiments, the heat convection coefficients of air approaching the housing were determined, since it is a complex geometry and analytically cannot be found. Furthermore, their model, can estimate thermally-induced preload, which is suitable for investigation of the thermal seizure failure of ball bearings. Boglietti A. et al [3], present a survey on the evolution and the modern approaches in thermal analysis of electrical machines and their inner components, including bearings, which are utilized in this research. In their work, the lumped parameter thermal network concept is described at detail, as well as numerical techniques including, computational fluid dynamics CFD and finite element methods FEM applied to thermal analysis. Nakajima K. [4], analyzed the thermal contact resistance between the balls and the inner and outer rings of a deep groove ball bearing subjected to axial loads, radial loads and a combination of both. Their findings show the relation of the thermal resistance and the applied load, the rotational speed and the contact angle.

Having said that, this paper presents a thermal model for determining the temperature distribution in a deep groove ball bearing model SKF 6303, subjected to radial loads within the range of $F_r = 0 - 1.7\,\text{kN}$ and a rotational speed within the range of $n = 0 - 1450\,\text{rpm}$. The representative model is divided into four control volumes, the housing, the outer-race, the balls and the inner-race. To create the lumped parameter thermal network, a concept widely utilized in electrical machines to determine their thermal behavior is applied in this work, the so-called light-gray box LPTN. The foundation and conceptualization of this methodology is extensively described in [5-6]. The main reason of applying this methodology lays on the possibility to model analytically the components of the representative model dividing them in a range of 5-15 nodes and the determination of the lumped parameters are based on the heat transfer theory. The nodes were meticulously selected, in order to enhance the calculations and the accuracy of the results. The thermal contact resistances are calculated as

functions of the frictional moment and heat losses. The energy equation is applied to each of the control volumes and its solution is obtained applying the state-space approach for the outer-race, balls and inner-race. In the case of the housing the analytical solution of the energy equation was solved as a non-homogeneous linear differential equation, since it is a static element and its initial condition could be determined by measurement. In this manner, the temperature fields of the housing T_h, outer-race T_o, balls T_b and inner-race T_i were calculated and were validated by experimental measurements obtained in an experimental bearing testing rig. The results are coherent since the deviation at the final time was less than 2.5 °C between the proposed thermal model and the experimental data.

2 Development of the thermal model

In this research, the development of the thermal model is divided into four stages, these are: load, friction, heat generation and state-space model as shown in Figure 1.

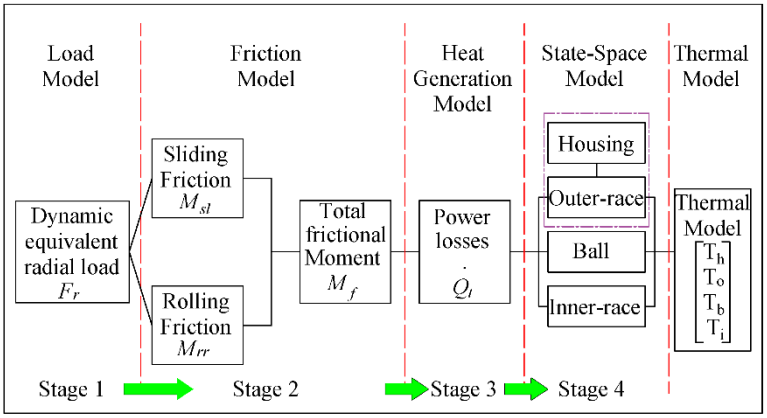

Fig.1. Stages of the thermal model. Load, friction, heat generation, State-Space model. (Source: Author).

2.1 Load Model

Primarily, deep groove ball bearings have more radial-carrying load capacity [7-8]. Therefore, it is not recommended for this type of bearings to be subjected to thrust loads. To assure that a ball bearing is subjected to radial load, the ratio f_c between the axial load F_a and the basic static load of the bearing C_o must be determined and the relation between the axial F_a and the radial load F_r must be less than $0.50\, f_c^{0.231}$.

Expanded information about the formulation of this relation can be found in [8]. Therefore, the dynamic equivalent radial load P_m is equal to the radial load as shown in Equation 1.

$$P_m = F_r = F_t \cdot \cos(\alpha) \qquad (1)$$

Where α is the contact angle and F_t is the total applied force.

2.2 Friction Model

Bearing friction is not constant and depends on diverse factors that occur due to the external loads applied to the bearings, the rotational speed and the lubrication conditions. In this

particular case, two main factors are considered, these are: sliding friction M_{sl} which depends on the type of lubrication and the rolling friction M_r, which enables the rotational movement, although simultaneously heat is dissipated. The manufacturers of bearings provide their own mathematical expressions to determine the total frictional moment. In this instance, the SKF frictional moment formulation is applied. Further details can be found in [1,9]. The total frictional moment was calculated applying Equation 2.

$$M_f = M_r + M_{sl} \tag{2}$$

Several values of the total frictional moment were calculated for different values of radial forces and within the established speed range and are shown in Figure 2.

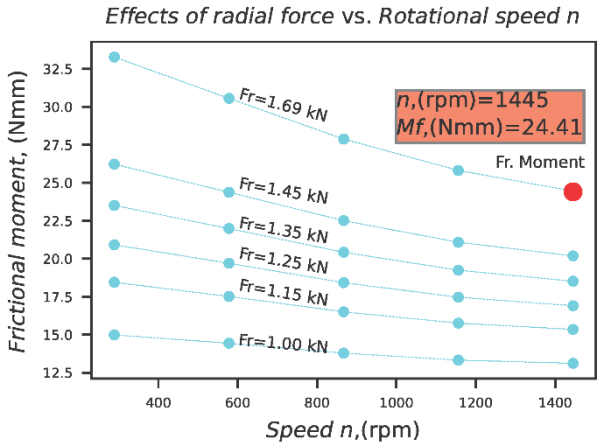

Fig.2. Total frictional moment M_f.

2.3 Heat Model

Heat is dissipated among the elements of the ball bearing (balls, inner- and outer-race) and the adjacent components (housing, shaft). The total heat losses Q_f depend on the total frictional moment and the rotational speed, and are determined using Equation 3.

$$Q_f = M_f \cdot n \tag{3}$$

The total heat loss Q_f, flows through the contact interfaces and is partitioned into the outer-race Q_{fo}, balls Q_b and inner-race Q_{fi} as shown in Equation 4.

$$\begin{aligned} Q_{fo} &= 0.25 \cdot Q_f \\ Q_{fb} &= 0.5 \cdot Q_f \\ Q_{fi} &= 0.25 \cdot Q_f \end{aligned} \tag{4}$$

Heat is dissipated by conduction due to friction contact between the outer-race and balls and inner-race and balls, obeying the laws of heat transfer theory [10]. The thermal resistances among the elements depend on the contact region generated when two surfaces interact. Generally, the contact region has an elliptic form and the determination of its major and minor axes a,b, respectively, are found applying Hertzian contact theory. In this work, the calculation of the thermal resistance R, between the contact regions is a function of the complete elliptic integral of the first kind $\psi(a/b)$, the major axis a and the thermal conductivity k of the elements. Hence, the thermal resistance is calculated using Equation 5.

$$R = \frac{\psi(a/b)}{k \cdot a} \tag{5}$$

Heat transfer by conduction is determined for the contact regions, these are: the inner-race and ball Q_{ib}, the balls and the outer-race Q_{ob}, the shaft and the inner-race Q_{is}. The formulation is given by Equation 6.

$$\begin{aligned} Q_{ib} &= \frac{(T_i - T_b)}{R_{ib}} \\ Q_{bo} &= \frac{(T_b - T_o)}{R_{bo}} \\ Q_{is} &= \frac{(T_i - T_s)}{R_{is}} \end{aligned} \tag{6}$$

Heat by convection is generated between the balls and the lubricant-film Q_{bl}, the outer-race and lubricant-film Q_{ol}, the inner-race and lubricant-film Q_{il} and between the housing and the surrounding air Q_{ha}. The heat convection coefficient of the lubricant h_l was calculated determining the Dean convection coefficient, which occurs between annular rings as in the present study. Extended details of the calculation and determination of the Dean flow phenomena can be found in [11-13]. The convection coefficient of air h_a was obtained from [14]. The formulation for the heat by convection is given by Equation 7.

$$\begin{aligned} Q_{bl} &= h_l \cdot (T_b - T_l) \\ Q_{ol} &= h_l \cdot (T_o - T_l) \\ Q_{il} &= h_l \cdot (T_i - T_l) \\ Q_{ha} &= h_a \cdot (T_h - T_a) \end{aligned} \tag{7}$$

The heat paths are depicted in Figure 3.

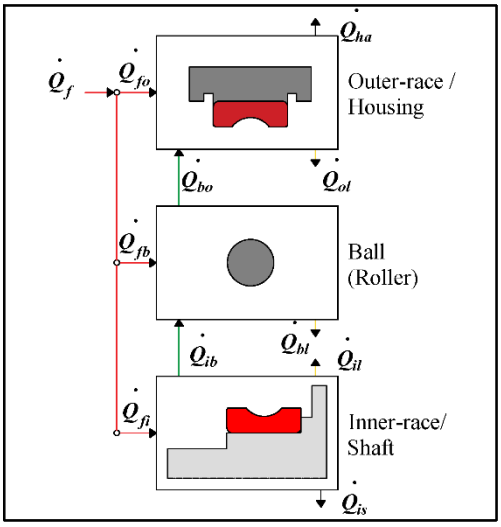

Fig.3. Heat flow distribution in the representative model. (Source: Author).

2.3.1 Lumped Parameter Thermal Network

A lumped parameter thermal network (LPTN) applying the light-gray box concept is implemented. The main reason for this creative approach is to find the diffusion nodes [6], thermal resistances, thermal paths and heat sources sufficient to describe the complete heat

transfer problem and apply heat transfer theory. On that account, 10 diffusion nodes, 3 heat sources and 9 thermal resistances were conceived. The lumped parameter thermal network is presented in Figure 4.

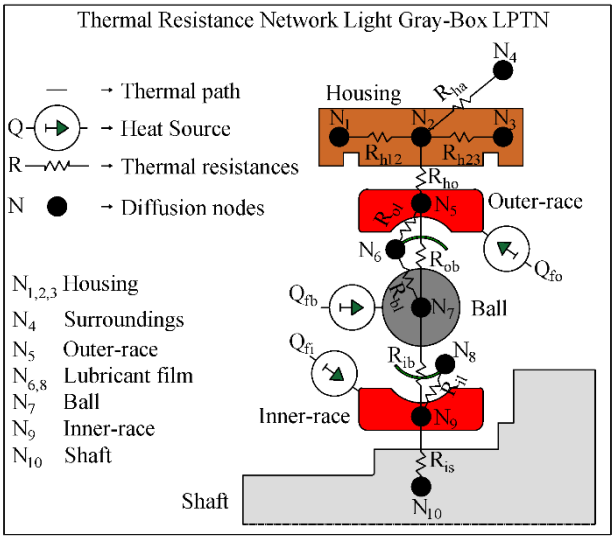

Fig.4. Lumped parameter thermal network using Light Gray-box approach. (Source: Author).

Employing the LPTN model and applying it to the four control volumes, the energy equation for the housing, outer-race, balls and inner-race is given in Equation 8.

$$\begin{aligned} m_h \cdot c_p \cdot \frac{\partial T_h}{\partial t} &= \dot{Q}_{oh} - \dot{Q}_{ha} \\ m_o \cdot c_p \cdot \frac{\partial T_o}{\partial t} &= \dot{Q}_{fo} + \dot{Q}_{bo} - \dot{Q}_{ol} \\ m_b \cdot c_p \cdot \frac{\partial T_b}{\partial t} &= \frac{1}{N}\dot{Q}_{fb} + \dot{Q}_{ib} - \dot{Q}_{bo} - \dot{Q}_{bl} \\ m_i \cdot c_p \cdot \frac{\partial T_i}{\partial t} &= \dot{Q}_{fi} - \dot{Q}_{ib} - \dot{Q}_{il} - \dot{Q}_{is} \end{aligned} \tag{8}$$

,where m_h, m_o, m_b, m_i , are the masses of the housing, outer-race, balls and inner-race, respectively. The number of balls is given by N and c_p is the specific heat.

2.4 State-Space Model

Equation 8, cannot be solved by conventional means, since there are more unknown variables than equations. Furthermore, these differential equations are linear non-homogenous equations, therefore, by traditional analytical methods, might be cumbersome to obtain a particular solution. In order to find a solution of Equation 8, the state-space approach is applied, considering that this system is linear time invariant, the inputs of the system Q_f , can be calculated from the external sources and that are sufficient conditions to determine the state-variables T_o, T_b, T_i of the system. A vast explanation about the usability and determination of state variables and the state approach is given by [15-16]. The state-space model of the system is given by Equation 9.

$$\begin{bmatrix} m_o c_p \dot{\bar{T}}_o \\ m_b c_p \dot{\bar{T}}_b \\ m_i c_p \dot{\bar{T}}_i \end{bmatrix} = \begin{bmatrix} \left(-\frac{1}{R_{bo}} - h_l \cdot A_o - \frac{1}{R_{oh}}\right) & \frac{1}{R_{bo}} & 0 \\ \frac{1}{R_{bo} \cdot N} & \frac{1}{N}\left(-\frac{1}{R_{ib}} - h_l \cdot A_b - \frac{1}{R_{bo}}\right) & \frac{1}{R_{ib} \cdot N} \\ 0 & \frac{1}{R_{ib}} & \left(-\frac{1}{R_{ib}} - h_l \cdot A_i - \frac{1}{R_{is}}\right) \end{bmatrix} \begin{bmatrix} T_o \\ T_b \\ T_i \end{bmatrix} + \begin{bmatrix} 0.25 \\ 0.5 \\ 0.25 \end{bmatrix} \sqcap Q_f \quad (9)$$

$$y = \begin{bmatrix} 1 & 0 & 0 \\ 0 & 1 & 0 \\ 0 & 0 & 1 \end{bmatrix} \begin{bmatrix} T_o \\ T_b \\ T_i \end{bmatrix}$$

,where A_b, A_i, A_o, are the convective surfaces of the ball, inner-race and outer-race respectively, the variable y, represents the output vector. In the case of the housing, the equation was solved as linear non-homogeneous differential equation, since it is possible to determine the initial conditions by experimental measurements. Therefore, it facilitates the determination of the particular solution, which was found using Equation 10.

$$T_h = \int (\sqcap_{oh} - \sqcap_{ha}) dt \qquad (10)$$
$$T_h(t=0) = Th$$

3 Results

The thermal model was solved and computed using MATLAB. The thermal properties and values of the coefficient involved in the calculation are given in Table 1. The geometrical characteristics of the Deep Groove Ball Bearing model 6303 SKF can be found in the catalogue of the manufacturer [17].

Table 1. Thermal properties of the ball Bearing.

Thermal Conductivity	$k = 46.6\,\mathrm{W/mK}$
Specific Heat	$c_p = 460\,\mathrm{J/kgK}$
Density	$\rho = 7860\,\mathrm{kg/m^3}$
Convective Coefficient of air	$h_l = 12.31\,\mathrm{W/m^2K}$
Convective Coefficient of the lubricant	$h_a = 409\,\mathrm{W/m^2K}$

The heat dissipation was calculated under the specified range of radial loads $F_r = 0 - 1.7\,\mathrm{kN}$ and within the rotational speed range $n = 0 - 1450\,\mathrm{rpm}$ which were chosen in accordance to the capabilities of the testing bearing rig wherein the thermal experiments were performed. The behavior of the total heat dissipation is depicted in Figure 5.

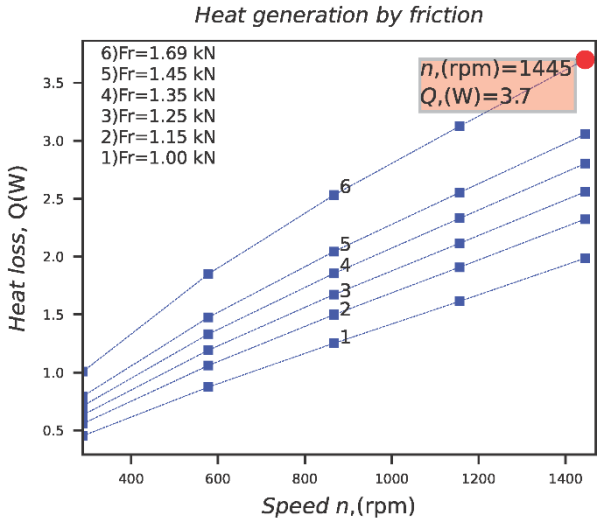

Fig.5. Total Heat losses $\overset{\sqcap}{Q}_f$.

3.1 Thermal experimental measurements

Experimental measurements were carried out employing an experimental bearing testing rig shown in Figure 6. The temperature of the non-movable parts (housing, outer-race, seal), were measured implementing four type K thermocouples, along with a thermal camera. The measurements obtained from the thermocouples were recorded by a thermal data logger. Six different values of radial loads shown Figure 5, were exerted over the housing by a hydraulic piston. The radial force was maintained constant during the specified time, as shown in Figure 7. The frequency of the electrical motor connected to the shaft of the bearing testing rig was set at $f = 25\,\text{Hz}$, resulting in $n = 1445\,\text{rpm}$ from the electrical motor.

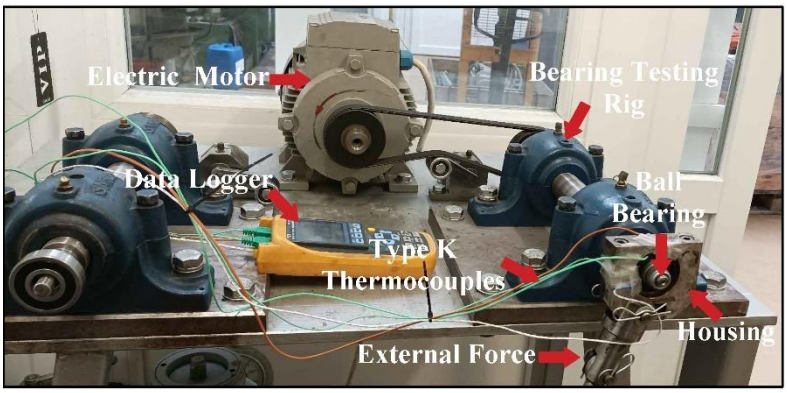

Fig.6. Experimental Bearing Testing Rig.

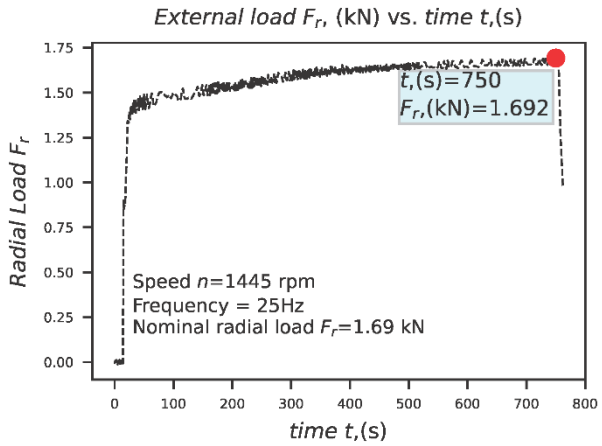

Fig.7. Radial Force $F_r = 1.69\,\text{kN}$ vs. time $t = 750\,\text{s}$.

3.2 Validation

The analytical solution of the thermal model has been compared with the experimental results for the housing and the outer-race. Subsequently, the predicted thermal behaviors of the ball and the inner-race were calculated. The thermometer YCT YC-747D wherewith the experimental measurements were obtained, possess an accuracy of $\pm(0.1\%\, rdg. + 0.7\,℃)$, a resolution of 0.1 ℃ and its range of measurement goes from $(-100\,℃\ to\ 400\,℃)$. Therefore, the instrumentation is appropriate in order to get accurate results.

3.2.1 Housing

Figure 8 depicts the thermal behavior of the housing. The initial condition $T_h(t=0) = 25.5\,°\text{C}$ was obtained from measurements at the beginning of the experiment. The experiment was conducted in a range of time equals to $t = 762\,\text{s}$. The analytical solution was determined solving Equation 10 for the same time period.

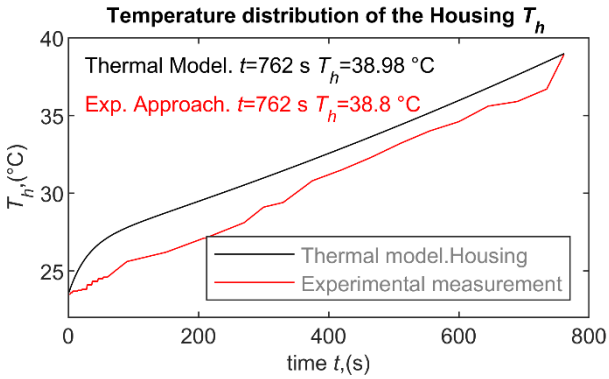

Fig.8. Temperature distribution of the housing T_h .

3.2.2 Outer-race

Figure 9, illustrates the thermal behavior of the outer-race. In this case, the state-variable T_o was calculated and the analytical and experimental analysis was performed during the same period of time as for the housing.

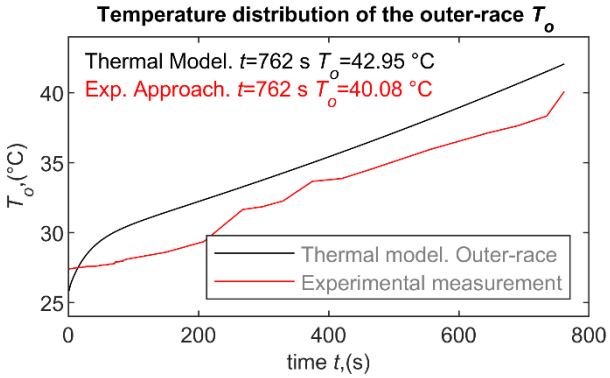

Fig.9. Temperature distribution of the outer-race T_o .

3.2.3 Ball

The thermal behavior of the ball, depends on the input variable $\overset{\sqcap}{Q}_f$, and the solution of the state-space model. Figure 10, illustrates the estimated thermal behavior of the balls.

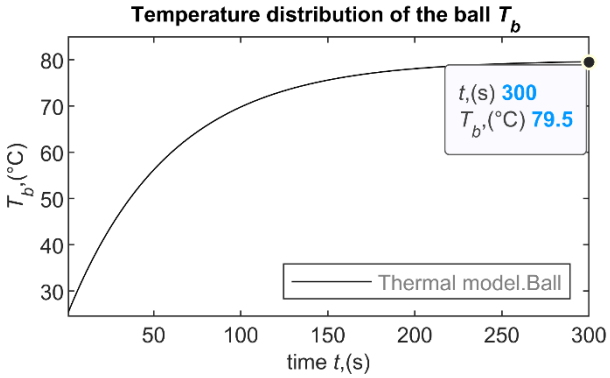

Fig.10. Temperature distribution of the ball T_b .

3.2.4 Inner-race

The thermal behavior of the inner-race is shown in Figure 11. The time of analysis is the same as utilized for the previous control volumes.

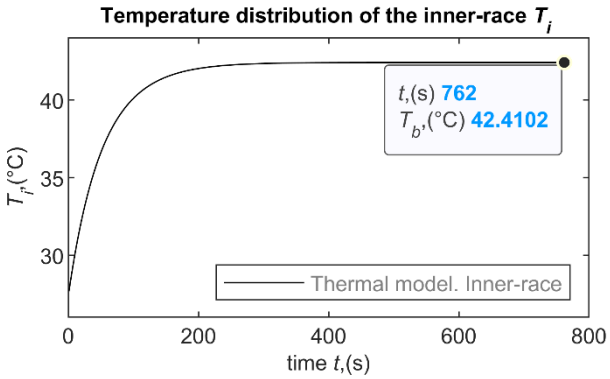

Fig.11. Temperature distribution of the inner-race T_i .

Table 2 presents a comparison between the thermal model and the experimental measurements for the housing and the outer-race, the mean standard deviation has been calculated to assess the agreement between the thermal model and the data.

Table 2. Temperature comparison of the experiments and the thermal model.

Control Volume	Initial Temperature °C		Final Temperature $t = 762\text{s}$ T(°C)		Increment ΔT		Deviation	
	Exp.	Th. Model	Exp.	Th. Model	Exp.	Th. Model	°C	%
Housing	23.50	23.50	38.80	38.98	15.30	15.48	0.13	0.33
Outer-race	26.50	28.00	40.08	42.95	13.58	14.95	2.03	5.06

4 Conclusions

In this research, a thermal model for a ball bearing subjected to radial loads was presented, applying the state-space approach and the Light Gray-Box lumped parameter thermal network. The Light Gray-Box LPTN methodology was selected aiming to obtain accurate results and establish appropriate thermal diffusion nodes. It could be observed that by the application of this methodology, sufficient parameters were determined, including the thermal resistances, heat sources and thermal paths. Three state-variables were chosen aiming to predict the thermal behavior of the bearing, these are: the temperature of the outer-race T_o, the temperature of the balls T_b and the temperature of the inner-race T_i . The input-variable of the system was the total heat flux $\dot{Q}_f$, which determination depends on the total frictional moment, the rotational speed and the applied external load. It could be seen that these variables are appropriate and enough to describe the heat transfer phenomena herein. The thermal behavior of the housing T_h was calculated apart from the state-space approach, since the descriptive parameters are simple to measure by observation. A particular solution of the non-homogenous linear differential equation describing the energy exchange of the housing was found. The presented thermal model has been validated by experimental measurements. During a range of time $t = 762\text{s}$, an increment of temperature equals to $\Delta T = 15.30°\text{C}$ and $\Delta T = 13.58°\text{C}$ occurred in the housing and outer-race respectively. The mean standard deviation of $sd = 0.33\%$ for the temperature distribution in the housing and $sd = 5.06\%$ for the outer-race was calculated. The temperature of the ball and the inner-race could not be

measured experimentally, since these elements are non-static, therefore is not feasible to get experimental results. Nevertheless, the proposed thermal model was able to foresee the temperature behavior of these elements. It could be seen that the predicted final temperature of the balls was $T_b = 79.5°C$. It is comprehensible, since the balls will absorb more heat from the total heat losses. In the case of the inner-race the final temperature was $T_i = 42.41°C$. Having said that, the presented model is in good agreement with the experimental measurements, therefore it can be applied to determine the thermal behavior in ball bearings of similar geometry. It is important to remark the model is controllable and observable, however, for this application it is only considered as an observer.

References

[1], F. Hoffmann, D. Silys and M. Doppelbauer, Transient Thermal Model for Ball Bearings in Electrical Machines, 2020 International Conference on Electrical Machines (ICEM), pp. 871-882, 2020, 10.1109/ICEM49940.2020.9270718.

[2], J. Takabi and M. M.Khonsari, Experimental Testing and Thermal Analysis of Ball Bearings, Springer Berlin, Heidelberg, vol.60, pp. 93-103, 2013, https://doi.org/10.1016/j.triboint.2012.10.009.

[3], A. Boglietti, A. Cavagnino, D. Staton, M. Shanel, M. Mueller and C. Mejuto, Evolution and Modern Approaches for Thermal Analysis of Electrical Machines, IEEE Transactions on Industrial Electronics, vol. 56 no.3, pp. 871-882, 2009, 10.1109/TIE.2008.2011622.

[4], K. Nakajima, Thermal Contact Resistance between Balls and Rings of a Bearing under Axial, Radial and Combined Loads, Journal of Themophysics and Heat Transfer, vol.9 no. 1, pp. 88-95, 1995, https://doi.org/10.2514/3.632.

[5], O. Wallschied and J. Böcker, Global Identification of a Low-Order Lumped Parameter Thermal Network for Pemanent Magnet Synchronous Motors, IEEE Transactions on Energy Conversion, vol.31 no. 1, pp. 354-365, 2016, 10.1109/TEC.2015.2473673.

[6], K & K Associates, Thermal Network Modelling Handbook, National Aeronautics and Space Administration, 2000.

[7], H. Nguyen-Schäfer, Computational Design of Rolling Bearings, Springer, 2016, https://doi.org/10.1007/978-3-319-27131-6.

[8], T. Harris and M. Kotzalas, Essential Concepts of Bearing Technology, Taylor & Francis, Fifth Edition, 2007.

[9], Y. R. Jeng and P.Y. Huang, Predictions of Temperature Rise for Ball Bearings, Tribology Transactions, vol.46 no.1, pp. 49-56, 2003, 10.1080/10402000308982599.

[10], T.L. Bergman and A.S. Lavine, Fundamentals of Heat and Mass Transfer, John Wiley & Sons, Eigth Edition, 2017.

[11], Y. Chen, H. Chen, J. Zhang and B. Zhang, Viscoelastic flow in rotating curved pipes, Physics of Fluids, vol.18 no. 8, pp. 279-300, 2006, 10.1063/1.2336454.

[12], H. Aoki, H. Nohira and H. Arai, Convective Heat Transfer in an Annulus with an Inner Rotating Cylinder, The Japan Society of Mechanical Engineers, vol.1967 no. 10, pp. 523-532, 1967, https://doi.org/10.1299/jsme1958.10.523.

[13], M. Khonsari and E.R. Booser, Applied Tribology: Bearing Design and Lubrication, John Wiley & Sons, Third Edition, 2017, 10.1002/9781118700280.

[14], S. Cabezas, G. Hegedus and P. Bencs, Transient heat convection analysis of a single rod in air cross-flow, Pollack Periodica, (to publish), 2023, 10.1556/606.2023.00768.

[15], D. H. Cooper, Hertzian Contact-Stress Deformation Coefficients, Journal of Applied Mechanics, vol.36 no. 2, pp. 296-303, 1969, https://doi.org/10.1115/1.3564624.

[16], M. Corinthios, Signals, Systems, Transforms, and Digital Signal Processing with MATLAB, CRC Press, 2009.

[17], SKF, SKF Catalogue, 2018, skf.com.